International Journal of Pharmaceutics 669 (2025) 125008

Contents lists available at ScienceDirect

International Journal of Pharmaceutics

journal homepage: www.elsevier.com/locate/ijpharm

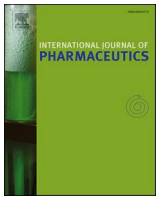

Harnessing osmotic shock for enhanced intracellular delivery of (nano) cargos

Beatrice Ruzzante [a], Flaminia Fruzzetti [a], Marco Cattaneo [b,c], Giuseppe Lauria Pinter [b,d], Stefania Marcuzzo [e,f], Gabriele Candiani [a,f], Nina Bono [a,*]

[a] genT_LAB, Dept. of Chemistry, Materials and Chemical Engineering "Giulio Natta", Politecnico di Milano, Milan, Italy
[b] ALS Centre, 3rd Neurology Unit, Fondazione IRCCS Istituto Neurologico "Carlo Besta", Milan, Italy
[c] Ph.D. Program in Pharmacological Biomolecular Sciences, Experimental and Clinical, University of Milan, Milan, Italy
[d] Department of Medical Biotechnology and Translational Medicine, University of Milan, Milan, Italy
[e] Neuroimmunology and Neuromuscular Diseases Unit, Fondazione IRCCS Istituto Neurologico "Carlo Besta", Milan, Italy
[f] Brain-targeted Nanotechnologies (BraiNs) Lab, Fondazione IRCCS Istituto Neurologico "Carlo Besta", Milan, Italy

ARTICLE INFO

Keywords:
Osmotic shock
Cell stimulation
Nanoparticles delivery
Drug delivery
Cell uptake
Cell volume

ABSTRACT

Efficient intracellular delivery of exogenous (nano)materials is critical for both research and therapeutic applications. The physicochemical properties of the cargo play a crucial role in determining internalization efficacy. Consequently, significant research efforts are focused on developing innovative and effective methodologies to optimize (nano)material delivery.

In this study, we utilized osmotic shock to enhance (nano)cargos internalization. We examined the effects of hypotonic/hypertonic shock on both primary and cell lines, assessing parameters such as cell viability, cell volume, membrane tension changes, and particle uptake. Our results indicate that short-lived osmotic shock does not harm cells. Hypotonic shock induced temporary shape changes lasting up to 5 min, followed by a 15-minute recovery period. Importantly, hypotonic shock increased the uptake of 100-nm and 500-nm particles by ~ 3- and ~ 5-fold, respectively, compared to isotonic conditions. In contrast, the hypertonic shock did not impact cell behavior or particle uptake.

Notably, the internalization mechanisms triggered by osmotic shock operate independently of active endocytic pathways, making hypotonic stimulation particularly beneficial for hard-to-treat cells. When primary fibroblasts derived from amyotrophic lateral sclerosis (ALS)-patients were exposed to hypotonic shock in the presence of the therapeutic cargo icerguastat, there was an increased expression of miR-106b-5p compared to isotonic conditions.

In conclusion, osmotic shock presents a promising strategy for improving drug delivery within cells and, potentially, in tissues such as muscles or skin, where localized drug administration is preferred.

1. Introduction

The intracellular delivery of exogenous (nano)materials has emerged as a crucial aspect of modern biology and biotechnologies, finding applications in genome-editing methodologies, *ex vivo* cell-based therapies, and various fundamental research endeavors (Morshedi Rad et al., 2021).

Over recent decades, researchers have devoted significant efforts to

Abbreviations: NP, (nano)particle; HeLa, human ovarian carcinoma epithelial cells; hFBs, human primary fibroblast cells; CTRL, control; PS, polystyrene; BCA, bicinchoninic acid; DMEM, Dulbecco's modified Eagle's medium; FBS, fetal bovine serum; cDMEM, complete DMEM; P/S, penicillin/streptomycin; dH_2O, deionized water; F, fluorescence; A, cell area; t, time; V, volume; k_b, Boltzmann constant; T, temperature; μ, binding free energy of the protein; a, membrane partition; σ, membrane tension; D_H, hydrodynamic diameter; ζ_P, zeta potential; P100, 100-nm particles; P500, 500-nm particles; DLS, dynamic light scattering; ELS, electrophoretic light scattering; PDI, polydispersity index; A, absorbance; RVD, regulatory volume decrease; RVI, regulatory volume increase; PTFE, polytetrafluoroethylene; ALS, amyotrophic lateral sclerosis; ALS-hFBs, hFBs from ALS patients.

* Corresponding author at: genT_LAB, Dept. of Chemistry, Materials and Chemical Engineering "G. Natta", Politecnico di Milano, Via Mancinelli 7 20131, Milan, Italy.

E-mail address: nina.bono@polimi.it (N. Bono).

https://doi.org/10.1016/j.ijpharm.2024.125008
Received 1 August 2024; Received in revised form 22 November 2024; Accepted 25 November 2024
Available online 4 December 2024

developing molecules and materials tailored for deployment within the intracellular *milieu*. These encompass a diverse array of substances, ranging from small molecules to nucleic acids such as DNA and RNA, proteins, synthetic nanomaterials like carbon nanotubes, quantum dots, nanoparticles, and microdevices, as well as experimental or therapeutic drugs (Gao et al., 2023; Morshedi Rad et al., 2021; Ray et al., 2017). Notably, these cargos exhibit considerable variability in size, shape, architecture, and chemical properties, which profoundly influence the efficacy of their internalization process, given the intrinsic impermeability of most cargos through cell membranes (Bono et al., 2020; Chou et al., 2011; Stewart et al., 2018; Zhang et al., 2023; Zhu et al., 2013). Although chemical and structural modifications can improve the membrane permeability of small molecules and short peptides, larger cargos require active intracellular delivery. This is achieved through a variety of delivery approaches that are classified based on how they pass through the plasma membrane. These approaches can be broadly categorized into two groups: (i) the use of carriers, wherein cargos are encapsulated within nano- and micro-particles that undergo uptake into endosomal trafficking routes or fuse with the target cell membrane, or (ii) physical methods leading to the transient disruption, destabilization, or permeation of the cell membrane to facilitate cargo entry (Stewart et al., 2018, 2016).

Carriers employed for the intracellular delivery of cargos encompass a wide array of biochemical systems ranging from molecular to nano- and micro-scale dimensions, such as synthetic and/or inorganic nanoparticles, molecular complexes, protein/peptide-based targeting agents, and bio-inspired systems incorporating elements of viral and bacterial origin. However, their effectiveness is often limited to specific subtypes.

Intracellular cargo delivery can also be accomplished through physical methods, which are promising options to carriers because they are applicable *in vitro* and *ex/in vivo*. These techniques and technologies rely on physical stimuli to entail transient disruptions in the plasma membrane through mechanical, electrical, thermal, optical, or chemical cues. These approaches can be broadly categorized into direct penetration and permeabilization means. Direct cell penetration relies on using a shaft or vehicle to breach the membrane and insert the cargo (e.g., microinjection, ballistic particles, and microneedles). Instead, permeabilization destabilizes the cell membrane to make it transiently porous and enable the entry of substances from the outside. Permeabilization strategies developed so far include electroporation, optoporation, cell squeezing, cavitation, thermal treatment, fluid shear stress, and osmotic shock (Stewart et al., 2016).

In this context, the quick alteration of osmotic pressure within cells emerges as a straightforward yet effective strategy to apply mechanical force to cell membranes, such as the plasma membrane and organelles (e.g., endosomes and pinosomes), and disrupt them (Stewart et al., 2018). However, achieving precise spatiotemporal control is challenging because altering media osmolarity can lead to significant cellular stress or death (Stewart et al., 2018).

In this study, we used osmotic shock to control cell membrane tension and improve the uptake of (nano)cargos. Plasma membrane tension arises from the combined contributions of osmotic pressure, in-plane tension, and cytoskeletal forces (Sitarska and Diz-Muñoz, 2020). Notably, the cytoskeleton plays a crucial role in most processes regulating membrane tension, such as cell volume (Fletcher and Mullins, 2010). When cells are exposed to hypotonic solutions, they swell, causing the plasma membrane to stretch and become more permeable (Adar et al., 2022; Dai et al., 1998; Fajrial et al., 2021; Mao et al., 2021; Pontes et al., 2017; Sinha et al., 2011; Thottacherry et al., 2018). On the other hand, exposure to hypertonic solutions causes cell shrinkage and reduces cell membrane tension (Adar et al., 2022; Ghisleni and Gauthier, 2024; Lang, 2007; Roffay et al., 2021; Venkova et al., 2022). In this context, it was hypothesized that these alterations in plasma membrane tension may ease the cell uptake of (nano)cargos, making osmotic shock a useful technique for controlling cell internalization. To shed more light on the relationship between osmotic shock and membrane tension, as well as the mechanisms involved in cell trafficking after osmotic shock, we devised a standardized protocol for subjecting cells to osmotic shock.

To ascertain how changes in environmental osmolarity affect cargo internalization, we first investigated the functional and morphological changes in cells exposed to hypotonic and hypertonic shocks. We then assessed the impact of osmotic shock on the internalization efficiency of fluorescent polystyrene (nano)particles (NPs) of varying sizes in a cell line and primary cells. Additionally, the effectiveness of this permeation strategy was evaluated in clinically relevant models *in vitro*, as demonstrated by the delivery of a therapeutic drug in a pre-clinical *in vitro* model of amyotrophic lateral sclerosis (ALS).

2. Experimental section

2.1. Materials

HeLa (human ovarian carcinoma epithelial cells, CCL-2) cell line was purchased from the American Type Culture Collection (ATCC®, Manassas, VA, USA), whereas human primary fibroblast cells (hFBs) were provided by Fondazione IRCCS Istituto Neurologico "Carlo Besta" (Milan, Italy). Specifically, cells were obtained from three ALS patients with bulbar onset meeting the diagnostic criteria for ALS (Brooks et al., 2000) and three healthy controls (CTRL) recruited at the Motor Neuron Disease Centre of the Fondazione IRCCS Istituto Neurologico "Carlo Besta". There were no differences in age, sex, and disease features within the ALS patient group and between patients and CTRL at the screening visit. Written informed consent was obtained from each subject.

Red fluorescent polystyrene (PS) particles (∅: 100 – 500 nm) were purchased from Magsphere Inc. (Pasadena, California, US). Bicinchoninic Acid (BCA) Protein Assay Kit and CellMask™ green plasma membrane stain, Universal PCR Master Mix TaqMan MicroRNA assays were from ThermoFisher Scientific (Monza, Italy). Alamar Blue Assay® was from Life Technologies (Monza, Italy). All other reagents were from Merck Life Science (Milan, Italy) unless otherwise specified.

2.2. Cell culture

Mycoplasma-free HeLa cells were cultured in Dulbecco's Modified Eagle's Medium (DMEM), supplemented with 10 % (v/v) fetal bovine serum (FBS), 1 mM sodium pyruvate, 10 mM HEPES, 100 U/mL penicillin, 0.1 mg/mL streptomycin, and 2 mM glutamine (hereinafter referred to as complete DMEM, cDMEM). hFBs were isolated from skin biopsies of three ALS patients with bulbar onset and three healthy CTRL, following a validated protocol (Varga et al., 2005). Cells were cultured in a proliferative medium, that is, DMEM supplemented with 20 % FBS, 1 % L-Glutamine, and 1 % penicillin/streptomycin (P/S). Cells were cultured at 37 °C in a humidified atmosphere under a constant supply of 5 % (v/v) CO_2 (hereafter referred to as standard culture conditions).

2.3. Preparation of media at a different osmolarity (tonicity)

Different media with varying osmolarity were prepared by diluting 15 % (v/v) cDMEM in 85 % (v/v) NaCl aqueous solutions (i.e., deionized water, dH_2O) at different salt concentrations (dilution factor: 1:5.6 (v/v)). For the experiments, hypotonic (< 330 mOsm/L) and hypertonic (>

Table 1
Composition of media at different osmolarity.

medium (100 µL)	cDMEM (µL)	NaCl (mg)	dH_2O (µL)
hypotonic (0.15×; 49.5 mOsm/L)	15	0.00	85
hypotonic (0.25×; 82.5 mOsm/L)	15	0.11	85
hypotonic (0.5×; 165 mOsm/L)	15	0.40	85
isotonic (1×; 330 mOsm/L)	15	0.96	85
hypertonic (2×; 660 mOsm/L)	15	2.10	85
hypertonic (3×; 990 mOsm/L)	15	3.23	85

330 mOsm/L) media were prepared as outlined in Table 1 and expressed as a function of the isotonic condition (1×). Of note, the isotonic medium had the same osmolarity (330 mOsm/L) of cDMEM. All media have equal cDMEM content.

2.4. Evaluation of osmotic shock on cell viability

To assess the optimal magnitude and duration of the osmotic shock, cell viability was assessed and compared to the standard culture conditions. Briefly, (adherent) HeLa cells were seeded onto 96-well plates at a density of 2×10^4 cells/cm^2 and maintained in standard culture conditions for 24 h. Afterward, fresh cDMEM was added to each well. After 30 min, cells were exposed to media with different osmolarity, namely 0.15× (~ 49.5 mOsm/L), 0.25× (~ 82.5 mOsm/L), 0.5× (~ 165 mOsm/L), 1× (~ 330 mOsm/L, CTRL), 2× (~ 660 mOsm/L), and 3× (~ 990 mOsm/L), then cells were incubated for different periods (i.e., 5 min, 15 min, 30 min, 1 h, 2 h, 4 h) in standard culture conditions. More specifically, the excess of cDMEM was removed from each well, and NaCl solutions (Table 1) were added and mixed through mild pipetting. Following the incubation in different media, osmolarity was adjusted to isotonic conditions by i) addition of NaCl in in sterile dH_2O for hypotonic conditions or ii) dilution in sterile dH_2O for hypertonic conditions. Cells were finally washed twice with cDMEM and then assayed with Alamar Blue® Cell Viability Assay directly or after a 24 h-incubation in standard culture conditions. Briefly, the medium was removed from each well and replaced with 100 µL/well of 1× resazurin dye solution in cDMEM. Next, plates were incubated in standard culture conditions for 2 h and the fluorescence recorded with a Synergy H1 reader (BioTek, Winooski, VT, USA) ($\lambda_{ex} = 540$ nm; $\lambda_{em} = 595$ nm). The viability of cells cultured in 1× isotonic medium was assigned to 100 % and the viability of cells cultured under hypotonic and hypertonic conditions was determined according to eq. (1):

$$Viability\ [\%] = \frac{F_{osmolarity}}{F_{isotonic,1\times}} \tag{1}$$

where F is the recorded fluorescence. During each step, special care was taken to avoid cell dehydration and shrinkage.

2.5. Evaluation of osmotic shock on cell morphology

2.5.1. Evaluation of cell area changes over time

To assess the impact of osmotic shock on cell morphology, changes in cell area (volume projection) following hypo- and hyper-tonic shocks were reckoned and compared to those of cells maintained in isotonic (1×) conditions. Briefly, cells were seeded onto 90-mm Petri dishes at a density of 1×10^4 cells/cm^2 and cultured under standard culture conditions for 24 h. Afterward, fresh cDMEM was added to each well. After a 30 min-incubation, cells were placed under a Zeiss Axioplan microscope and exposed to media with different osmolarity, specifically 0.15× (~ 49.5 mOsm/L) and 3× (~ 990 mOsm/L). Bright-field live videos were recorded for 30 min at 80× magnification. Recordings started before osmotic shock to take images of cells in standard conditions. For each condition, videos were analyzed using a custom MATLAB® code (see Supplementary Material S1). Briefly, for each frame, the area of individual cells was manually selected, and the variation of cell area over time was expressed as a function of the initial area (eq. (2):

$$cell\ area\ variation = \frac{A_t}{A_{t=0}} \tag{2}$$

For each frame, values of cell area variations were averaged, and changes in cell area over time were computed as follows (eq. (3):

$$relative\ area\ change = \frac{\left(\frac{A_t}{A_{t=0}}\right)_{tested\ \ osmolarity}}{\left(\frac{A_t}{A_{t=0}}\right)_{isotonic,1\times}} \tag{3}$$

2.5.2. Analysis of cell volume measurements upon osmotic shock

To assess single-cell volume changes over time after osmotic shock, we utilized the method by Urbaniak et al. that allows estimating the 3D cell shape from 2D images (Urbaniak et al., 2022). Briefly, 2D images were taken from the frames of cell videos, as described in section 2.5.1. In every frame, the thickness of each cell was determined by analyzing the gray values of the cell. The volume of single cells was then calculated as the sum of the gray values within its area. Finally, the volume change of each cell over time was computed according to eq. (4):

$$relative\ single\ cell\ volume\ variation = \frac{V_t}{V_{t=0}} \tag{4}$$

where t is the time, V_t is the volume variation with respect to the volume at t = 0. For a thorough description of the method, refer to **Supplementary Materials S1**.

2.5.3. Mathematical model of cell membrane tension changes upon osmotic shock

To assess the temporal changes in cell membrane tension following osmotic shock, we employed the model proposed by Roffay et al. (Roffay et al., 2021). Briefly, the variation of membrane tension was computed according to (eq. (5).

$$\sigma_t = \frac{k_b T}{a} \log\left(\frac{\left(2\left(\frac{V(t)}{V_0}\right)^{\frac{2}{3}} - 1\right) e^{\frac{\mu}{k_b T}}}{\left(\frac{V(t)}{V_0}\right)^{\frac{2}{3}} e^{\left(\frac{\mu}{k_b T} - \frac{a\sigma_0}{k_b T}\right)} + 1 - \left(\frac{V(t)}{V_0}\right)^{\frac{2}{3}}} \right) \tag{5}$$

where t is the time, $V(t)$ is the volume variation with respect to the volume at t = 0 in isotonic conditions V_0, k_b (1.38×10^{-23} J/K) is the Boltzmann constant, T is the temperature, μ is the binding free energy of the protein, a is the membrane partition, σ_0 is the membrane tension at t = 0 in isotonic conditions, and σ is the membrane tension at t. The values of σ_0 (1.2×10^{-4}N/m), μ (1.5 k_bT), and a (53 nm^2) utilized in this study, and relative to HeLa cells, were taken from the literature (Roffay et al., 2021).

The volume variations obtained as described above were fitted into the equation to determine the variation of membrane tension over time, calculated according to eq. (6):

$$relative\ membrane\ tension\ variation = \frac{\sigma_t}{\sigma_0} \tag{6}$$

For a comprehensive description of the derivation model, refer to Supplementary Materials S2.

2.6. Evaluation of osmolarity shock on cell uptake

2.6.1. Evaluation of particles characteristics upon resuspension in different media

2.6.1.1. Evaluation of physicochemical characteristics of particles in different media. To evaluate the effects of different media on the physicochemical characteristics of particles, their size, expressed in terms of hydrodynamic diameter (D_H), and the overall surface charge, expressed in terms of zeta potential (ζ_P), were evaluated. Briefly, aqueous suspensions of particles of nominal 100 nm diameter (P100) and 500 nm diameter (P500) were sonicated for 10 min with a bath sonicator and promptly re-suspended in media with different osmolarity, namely

dH_2O, 0.15× hypotonic medium, 1× isotonic medium, and 3× hypertonic medium, at a final concentration of 100 μg/mL. Then, the D_H and the ζ_P were evaluated at room temperature (r.t.) through Dynamic Light Scattering (DLS) and Electrophoretic Light Scattering (ELS), respectively, using a Malvern Zetasizer Nano ZS instrument (Malvern, UK), fitted with a 5 mV HeNe laser ($\lambda = 633$ nm) and a scattering angle of 173°.

To assess whether particles aggregate over time, the D_H and the Polydispersity Index (PDI) were assessed 0, 30 min, 1 h, 2 h, 3 h, and 4 h post-resuspension.

2.6.1.2. Evaluation of particle settling in different media. To assess whether particles settled during the timeframe of the experiment and to examine the dependence on resuspension media, UV–vis spectrophotometric analyses were carried out (Zheng et al., 2019). Briefly, P100 and P500 were sonicated and resuspended as described herein above. Then, the absorbance of the particle suspension was measured at r.t. in a V-630 UV–vis spectrometer (Jasco, Cremella (Lc), Italy) ($\lambda_{max} = 250$ nm) every minute for 4 h. The sedimentation was evaluated through the variation of absorbance over time (A_t/A_0), where A_0 was the absorbance at time 0 and A_t was the absorbance at a given time t.

2.6.2. Evaluation of particle uptake in cells upon osmotic shock in upward set-up

To evaluate the effects of osmolarity shock on particle uptake, HeLa cells, and hFBs were seeded onto separate wells of a 12-well plate at a density of 2×10^4 cells/cm^2 and maintained in standard culture conditions for 24 h.

Following incubation, cells were challenged with P100 or P500 resuspended in different media (0.15× hypotonic medium, 1× isotonic medium, and 3× hypertonic medium) at a final concentration of 100 μg/mL, as described herein above. Cells were incubated with particles for 30 min in standard culture conditions. Cells incubated without particles were used as the blank. To evaluate the internalization efficiency, following 30-min incubation, cells were washed three times (each well with its specific particle-free media) and lysed. The fluorescence of cell lysates was read using a Synergy H1 reader ($\lambda_{ex} = 538$ nm; $\lambda_{em} = 584$ nm). For each condition, the fold-change in particle uptake as compared to cells cultured in 1× isotonic medium was calculated as follows (eq. (7):

$$fold\ change = \frac{F_{sample} - F_{blank}}{F_{isotonic,1\times} - F_{blank}} \quad (7)$$

2.7. Evaluation of particle uptake in cells in pre- and post-swelling conditions

Experiments on particle uptake were performed in pre- and post-swelling conditions to shed light on the mechanism behind particle uptake upon hypotonic shock. Experiments were performed following the same protocol described herein above. HeLa cells were seeded onto a 12-well plate at a density of 2×10^4 cells/cm^2 and maintained in standard culture conditions for 24 h. In the post-swelling condition, cells were challenged with P500 at a final concentration of 100 μg/mL, resuspended in different media (0.15× hypotonic medium, 1× isotonic medium), while in the pre-swelling condition, P500 were dripped 5 min after the administration of osmotic shock (0.15× hypotonic medium, 1× isotonic medium). Cells were incubated in standard cell culture conditions in the pre- and post-swelling conditions with particles for 30 min, while the osmotic shock was kept for 30 min in both conditions. Cells incubated without particles were used as controls. To evaluate the internalization efficiency, cells were washed three times (each well with its specific particle-free media) and lysed. The fluorescence of cell lysates was read with a Synergy H1 reader ($\lambda_{ex} = 538$ nm; $\lambda_{em} = 584$ nm). For each condition, the fold-change of particle uptake was calculated according to eq. (7).

2.8. Evaluation of particle uptake in cells upon osmotic shock at 4 °C

Experiments were performed following the same protocol described in Section 2.7. HeLa cells were seeded onto a 12-well plate at a density of 2×10^4 cells/cm^2 and maintained in standard culture conditions for 24 h. Following incubation, cells were challenged with P500 that were resuspended in different media (0.15× hypotonic medium, 1× isotonic medium) at a final concentration of 100 μg/mL. Cells were incubated with P500 particles for 30 min at 4°C and 37°C (controls). To evaluate the internalization efficiency following 30-min incubation, cells were washed three times (each well with its specific particle-free media) and lysed. The fluorescence of cell lysates was read with a Synergy H1 reader ($\lambda_{ex} = 538$ nm; $\lambda_{em} = 584$ nm). For each condition, the fold-change of particle uptake was computed according to eq. (7). Cell viability was evaluated as described in Section 2.4 and calculated according to eq. (1).

2.9. Evaluation of particle uptake in cells upon osmotic shock in upside-down set-up

Experiments were performed using a set-up already published (Pezzoli et al., 2017). Briefly, three polytetrafluoroethylene (PTFE) cylindrical spacers (height 2 mm, diameter 1.5 mm) were glued on the surface of 9.8 mm diameter glass coverslips using Silastic® Medical Adhesive Silicone Type A (Dow Corning, Auburn, MI, USA). After overnight incubation to allow the glue to polymerize and dry, the coverslips were poured into pure ethanol (30 min) and sterilized under UV irradiation (15 W germicidal lamp, 30 min). Coverslips were placed upward in 24-well plates (with the spacers facing upward) and cells were seeded. Twenty-four h post-seeding, coverslips were turned upside-down, with cells facing the bottom of the well. Coverslips seeded with cells and placed upright in wells with no particles were used as controls. Cellular uptake experiments were performed according to the protocol described in Section 2.7.

2.10. Evaluation of therapeutic molecules uptake in cells upon osmotic shock

hBFs cells isolated from ALS patients (ALS-hBFs) and healthy CTRL cells were seeded onto separate wells of a 12-well plate at a density of 3×10^4 cells/mL and maintained in standard culture conditions for 24 h. ALS-hBFs were next challenged with icerguastat, a neuroprotective compound acting through the unfolding protein response modulatory mechanisms, dissolved in 0.15× hypotonic and 1× isotonic medium at a final concentration of 10 nM (Vieira et al., 2015). Cells were incubated with the drug for 30 min in standard culture conditions. ALS-hBFs cultured in standard culture media (without the drug) were used as the basal control, while CTRL cells were used as the reference.

Following a 30-min incubation, cells were washed with fresh culture medium and cultured for additional 71.5 h in standard culture conditions before being collected for molecular analysis. Total RNA was extracted with Trizol reagent from hFIBs and reverse-transcribed to cDNA using TaqMan microRNA Reverse Transcription Kit with specific primers for miR-106b-5p and U6. cDNA aliquots corresponding to 15 ng total RNA were amplified by quantitative real-time PCR in duplicate from three different and independent experiments with Universal PCR Master Mix and specific predesigned TaqMan MicroRNA assays (Thermo Fisher Scientific). miRNA levels normalized to U6 were expressed using the $2^{-\Delta Ct}$ formula, During the tests, miR-106b-5p were used as the biomarker for the response to icerguastat in ALS patients with bulbar onset, according to a patent (Marcuzzo et al., 2024). U6, stably expressed across ALS and CTRL hFBs, was used as the endogenous control for data normalization.

2.11. Statistical analysis

Statistical analyses were carried out using Prism version 8

(GraphPad, La Jolla, CA, USA). Data were initially analyzed using normality test. The unpaired *t*-test and Kolmogorov-Smirnov test were used to compare two experimental groups. Significance was retained when $p < 0.05$. Data are expressed as mean ± standard deviation (SD, $n \geq 3$) unless differently specified.

3. Results and discussion

Transporting molecules and (nano)materials into cells is a crucial aspect of decoding cell function, guiding cell fate, and reprogramming cell behavior. Scientists focus on intracellular delivery to transport diverse types of cargo for various applications. The cargos can vary significantly in size, shape, architecture, and chemical properties, as they span from small hydrophilic molecules, about 1 nm in size, to large organelles and microorganisms that are microns in size.

In this work, we identified osmotic shock as a means to increase the internalization efficiency of cargos in the form of small therapeutic molecules (IF-088, Ø < 1 nm) and nano-sized particles (P100 and P500).

The application of osmotic shock to cells is a straightforward and cost-effective way to overcome the cell membrane barrier and enhance the cellular uptake of cargo. Despite historical use, unfortunately, this approach has not been fully exploited yet. This is because of the major hurdles in achieving precise spatiotemporal control of the stimulus, leading to significant variability in experimental outcomes, and given the limited understanding of the mechanisms underlying cell perturbation and cargo uptake (Stewart et al., 2018).

Notably, two main approaches typically reported in literature studies are i) the dilution of the culture medium in dH_2O to induce hypotonic shock (Guo et al., 2017; Model et al., 2022; Roffay et al., 2021), and ii) the addition of cell-impermeant osmolytes (such as salt (Biswas et al.,

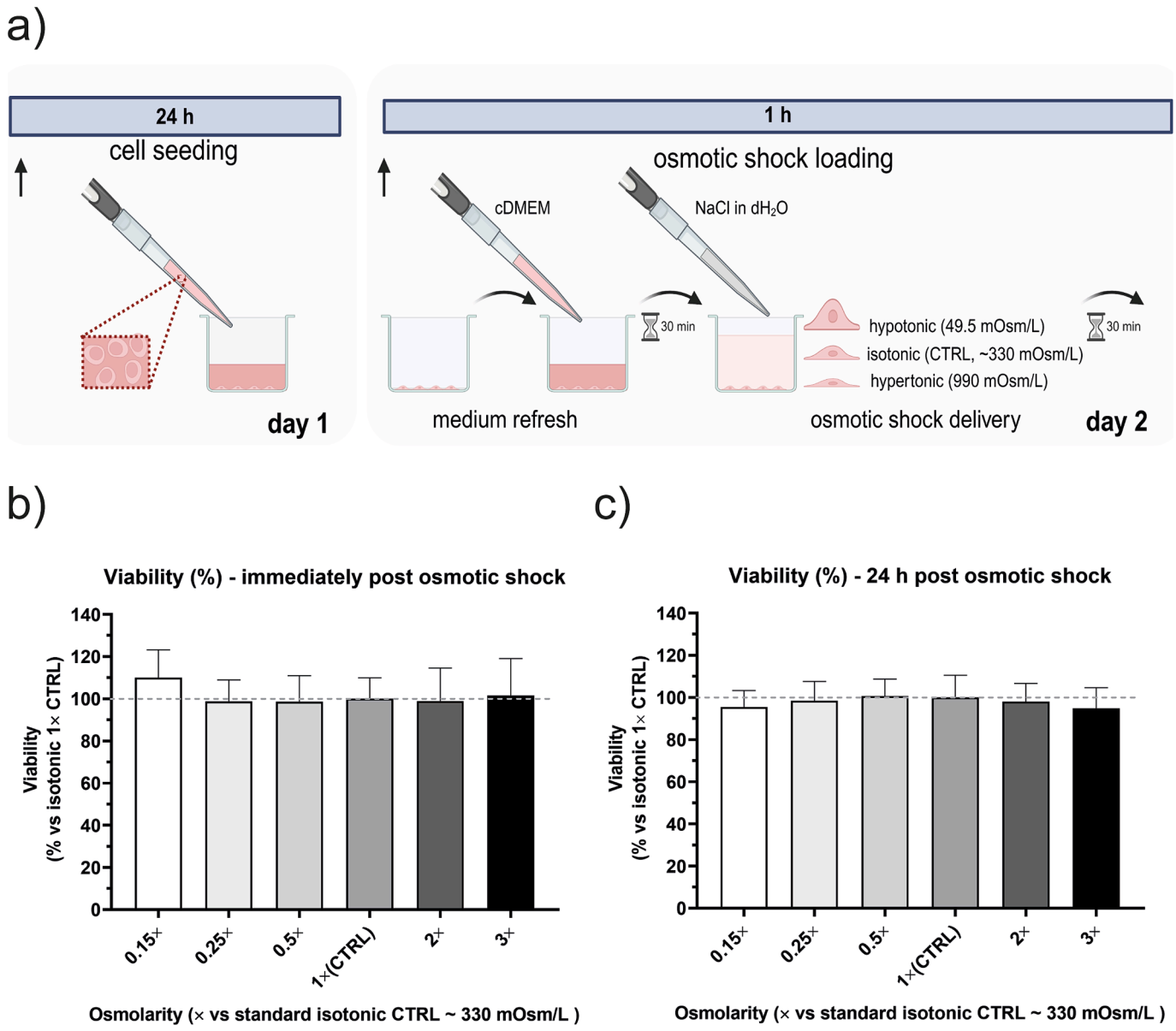

Fig. 1. a) Workflow of the osmotic shock experimentation. Twenty-four h after seeding, the culture medium was replaced with warm cDMEM. Next, cells were incubated in standard conditions for 30 min to let cells recover from medium change shock. Afterward, cells were challenged with media with different osmolarity for 30 min, through the addition of a solution of NaCl in sterile dH_2O to the culture medium present in each well. All media had the same cDMEM content (i.e., 15 % v/v, cDMEM osmolarity ~ 330 mOsm/L), and osmolarity variations were achieved by adjusting the concentration of NaCl in the medium. (Image created with Biorender.com). **b)** Assessment of HeLa cell viability after the osmotic treatment, and **c)** after 24 h using the Alamar Blue® Viability assay. Results are expressed as mean ± SD ($n \geq 6$) (*$p < 0.05$). (For interpretation of the references to colour in this figure legend, the reader is referred to the web version of this article.)

2022; Guilak et al., 2002; Holst et al., 2017) or sugars (Ayee et al., 2018; Peckys and Mazur, 2012; Roffay et al., 2021)) to obtain high-osmolarity solutions. However, in these investigations, modification of specific ion content or additive concentrations (e.g., FBS) in the medium could have potentially impacted the outcomes. To tackle this issue, we have devised a reliable protocol (Fig. 1**a**) that considers maintaining consistent medium additive concentrations across all experimental conditions to ensure highly reproducible results. In this context, variations in cell behavior solely rely on the medium osmolarity.

3.1. Cell viability and cell volume changes in response to osmotic shock

To assess the cell response to osmotic shock, we initially confirmed the absence of any harmful or cytotoxic effect associated with this kind of stimulation (Ponti et al., 2022). Various types of osmotic shock were applied to HeLa cells for different durations, including 5 min, 15 min, 30 min, 1 h, 2 h, and 4 h. Interestingly, no changes in cell viability were observed up to 30 min of stimulation (data not shown), regardless of the osmotic shock applied. As a result, we deliberately chose a 30-min stimulation period for our investigation.

It is worth noting that any mechanical or chemical stimulus may

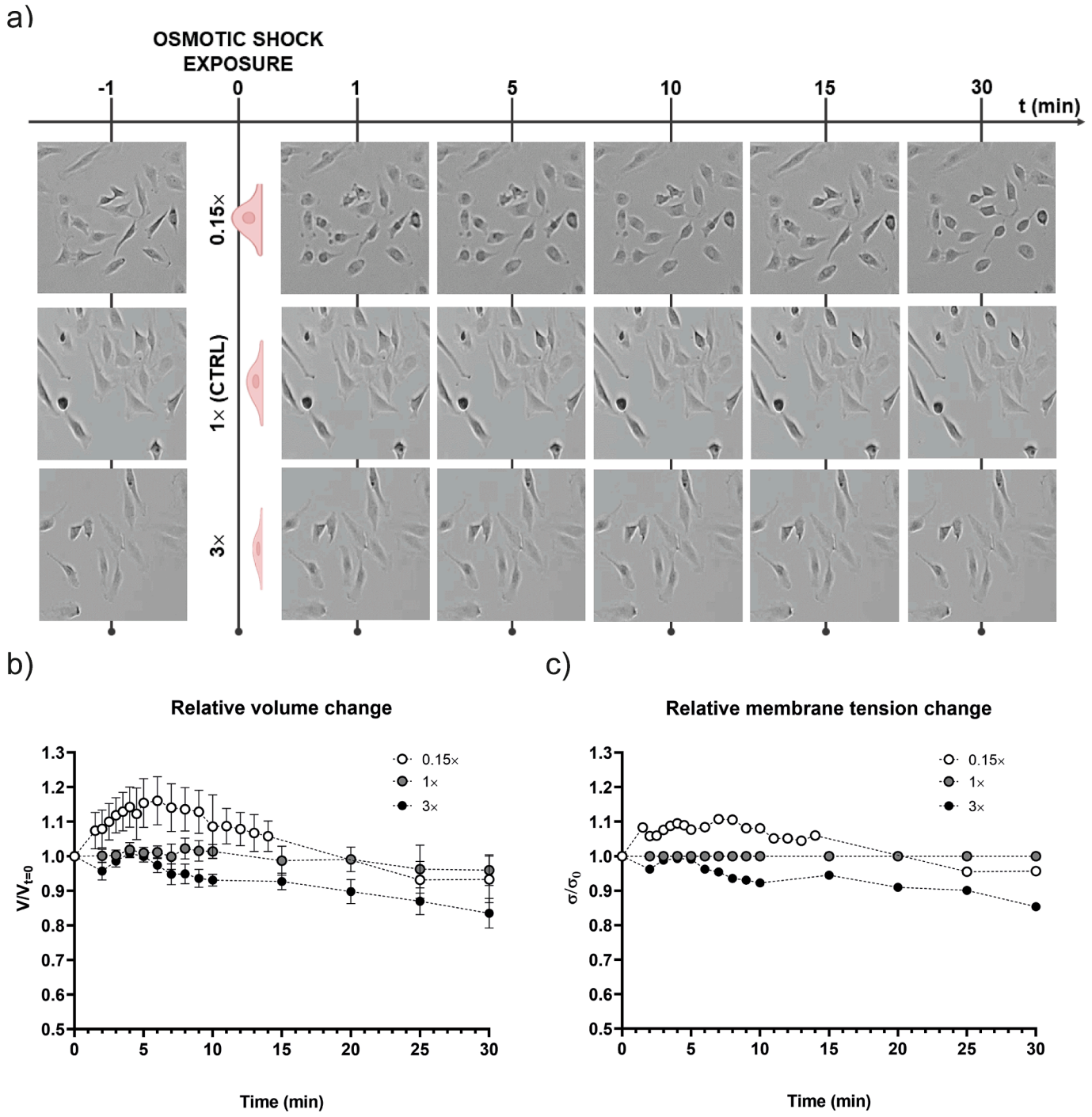

Fig. 2. a) Morphological analysis of HeLa cells exposed to hypotonic (0.15×), isotonic (1×, CTRL), and hypertonic (3×) *milieus*. **b)** Evaluation of cell volume changes over time. Data are expressed as mean ± C.I., 95 % (n ≥ 10). **c)** Mathematical derivation of membrane tension changes over time.

cause some cell stress response, potentially triggering cell behavior changes. Therefore, we checked for possible changes in cell proliferation rate following a 30-min long osmotic shock, thus expanding our investigation on the effects of osmotic shock.

To the best of our knowledge, this is one of the very few studies in which cells are exposed to such a severe osmotic shock for an extended duration (Model et al., 2022; Peckys and Mazur, 2012; Venkova et al., 2022). Indeed, cells are typically stimulated, and the effects are assessed, over shorter times, up to 15 min (Ayee et al., 2018; Diz-Muñoz et al., 2016; Fajrial et al., 2021; Guo et al., 2017; Holst et al., 2017; Kaplan et al., 2022; Lin and Liu, 2019; Loh et al., 2019; Pan et al., 2019; Roffay et al., 2021; Takai and Ohmori, 1990; Thottacherry et al., 2018). However, these endpoints are far from drug delivery kinetics that require the uptake of nanomaterials (Gratton et al., 2008; Mann et al., 2016). In our study, neither hypotonic nor hypertonic media adversely affected cell viability or proliferation immediately after stimulation (Fig. 1**b**) or 24 hours later (Fig. 1**c**) ($p > 0.05$). Therefore, the osmotic conditions of 0.15× and 3× were selected for subsequent experiments.

In vivo and when cultured *in vitro,* most mammalian cells thrive in a 270–330 mOsm/L aqueous environment (Mang et al., 2020; Ozturk and Palsson, 1991; Sieber et al., 2020; Xu et al., 2010). Variations of this condition induce notable changes in cell volume, morphology, and functioning (Roffay et al., 2021; Venkova et al., 2022). Indeed, when exposed to a low-osmolarity solution, cells undergo hypotonic swelling as a result of the water influx with the dissolved solutes through the plasma membrane (Adar et al., 2022). Conversely, exposure to a high-osmolarity medium results in hypertonic cell shrinkage (Lang, 2007). In this sstudy, live cell imaging was performed over a 30-min time window to observe and characterize morphological changes (**Supporting Information Videos 1–3**). As expected, cells exposed to hypotonic (0.15×) and hypertonic (3×) environments underwent morphological modifications, whereas no changes were observed when incubated in isotonic media (1×). Fig. 2**a** shows different timeframes representative of the two behaviors.

We quantified these changes by measuring the 2D cell area variations over time of 3D cell volume projections. We segmented time-lapse videos using a custom MATLAB code and extracted the cell area. Subsequently, we correlated these data with cell volume information. Image reconstruction was carried out using the method outlined by Urbaniak *et al.* to estimate 3D cell shape from 2D pictures (Urbaniak et al., 2022) (**Figure S1a**, and **Supporting Information Videos 4–6**), and relative cell volumes were extracted.

Cells incubated in the 0.15× medium exhibited an abrupt ~ 15 % increase in volume (Fig. 2**b**) and area (**Figure S2**) in the first 5 min of hypotonic shock, followed by a steady recovery to the initial level (i.e., isotonic condition). Conversely, the 3× hypertonic medium led to slight and steady volume and area reductions over the entire duration of the experiment. The existing literature reports changes in volume within minutes of stimulation, which aligns well with these findings (Fajrial et al., 2021; Hoffmann et al., 2009; Model et al., 2022; Peckys and Mazur, 2012; Roffay et al., 2021; Sinha et al., 2011; Venkova et al., 2022). Besides, there is extensive literature regarding cell volume recovery as a consequence of the hypotonic treatment. This restorative process, collectively known as Regulatory Volume Decrease (RVD), is caused by the osmolyte release (primarily potassium and chloride) and compensatory cell shrinkage in response to abrupt cell swelling (Alexander and Grinstein, 2006; Lang, 2007). Essentially, cells take advantage of active regulatory volume mechanisms to counteract the increase in cell surface area/volume, which could otherwise lead to severe cell damage and eventually death (Adar et al., 2022). Conversely, cells exposed to hypertonic treatment experience a gradual decrease in cell volume. Although an opposing mechanism for cell volume regulation in hypertonic conditions exists, called regulatory volume increase (RVI), HeLa cells do not necessarily recover from hypertonic shock, as previously reported (Roffay et al., 2021).

Cells actively regulate their volume in response to osmotic challenges, followed by passive adjustments in plasma membrane tension. To explore the interplay between these two factors, we extrapolated membrane tension variations as a function of cell volume changes according to Roffay *et al.* (Roffay et al., 2021). As depicted in Fig. 2**c**, during the the post-osmotic shock period, cell volume varies to equalize osmotic pressures inside and outside the cell, with membrane tension dynamically adapting to these fluctuations. Overall, the hypotonic shock induced an abrupt rise in membrane tension (~10 % variation), whereas the hypertonic shock resulted in a stepwise reduction of membrane tension to a similar extent. These observations disclose that membrane tension passively adapts to volume changes throughout the response to and the recovery from osmotic shocks, as already reported in the literature (Diz-Muñoz et al., 2016; Roffay et al., 2021).

One core question raised by the tight coupling of membrane tension variations and volume changes during osmotic shocks is whether and how these phenomena control the intracellular delivery of extracellular cargoes.

3.2. Hypotonic shock to cells increases NPs uptake

The control of the osmotic homeostasis is crucial for cellular functions, leading to the activation of various mechanisms to counteract disturbances in cell volume. In addition, a hypotonic extracellular medium causes cell swelling and heightened membrane tension, while hypertonic conditions induce cell shrinkage and reduced membrane tension. As endocytosis involves plasma membrane remodeling, we hypothesized that stimuli affecting plasma membrane tension may impact internalization efficiency (Akatay et al., 2022; Boulant et al., 2011; Djakbarova et al., 2021; Gauthier et al., 2012; López-Hernández et al., 2020; Mao et al., 2021; Pontes et al., 2017; Sinha et al., 2011; Thottacherry et al., 2018).

To investigate the impact of osmotic shock on cargo internalization, we utilized fluorescent PS particles in two size ranges (nominal diameter: 100 – 500 nm). The NPs sizes were intentionally selected to match those of existing therapeutics such as lipid- and polymer-based nanoparticles and drug-loaded liposomes (Fröhlich et al., 2009; Lunov et al., 2011; Monti et al., 2015; Nowak et al., 2020; Stewart et al., 2018). We first questioned whether different osmotic media would affect the physicochemical characteristics and behavior of P100 and P500 (e.g., size, surface charge, aggregation, sedimentation) over time. It is apparent from Table 2 that the D_H of P100 and P500 particles suspended in media of different tonicity were invariably similar ($p > 0.05$).

Furthermore, both kinds of particles displayed slightly negative surface charges ranging between −10 and −15 mV (**Figure S3c**). The

Table 2
Physicochemical characteristics of PS particles suspended in different media. 'Fresh' means that D_H and Polydispersity Index (PDI) of particles were analyzed immediately after suspension in media at different osmolarity, whereas '4h' indicates particle features measured 4 h after suspension.

P100	**fresh**		**4 h**	
medium	**D_H (nm)**	**PDI**	**D_H (nm)**	**PDI**
hypotonic (0.15×; 49.5 mOsm/L)	170 ± 10.4	0.15 ± 0.01	185 ± 4.3	0.16 ± 0.02
isotonic (1×; 330 mOsm/L)	133 ± 0.2	0.05 ± 0.01	131 ± 5.4	0.05 ± 0.04
hypertonic (3×; 990 mOsm/L)	130 ± 2.0	0.06 ± 0.01	129 ± 1.7	0.04 ± 0.03
P500	**fresh**		**4 h**	
medium	**D_H (nm)**	**PDI**	**D_H (nm)**	**PDI**
hypotonic (0.15×; 49.5 mOsm/L)	763 ± 20.9	0.05 ± 0.05	644 ± 3.4	0.05 ± 0.06
isotonic (1×; 330 mOsm/L)	605 ± 7.8	0.08 ± 0.07	615 ± 5.3	0.03 ± 0.04
hypertonic (3×; 990 mOsm/L)	639 ± 19.4	0.17 ± 0.12	683 ± 8.0	0.12 ± 0.07

slight discrepancy in the measured particle size with respect to their nominal size (measured in dH_2O as reported in **Figure S3a-b**) may be related to the formation of a protein corona in the presence of cDMEM in each of those exposure media (Corbo et al., 2016; Zanganeh et al., 2016).

Of note, both P100 and P500 retained their characteristics throughout the entire 4-h time-lapse (Table 1 and **Figure S2a-b**). Neither aggregation nor sedimentation was observed during the experiments, as demonstrated by the low PDIs reported in Table 2 and data displayed in **Figures S3a-b**.

First, we assessed whether P100 and P500 were internalized by cells within a 30-min timeframe. As expected, both P100 and P500 particles were internalized by cells; however, the uptake of P500 was less efficient compared to that of smaller particles (Figure S4). This phenomenon may be ascribed to the greater mechanical stress exerted on the cell membrane by the larger P500 nm particles, which typically resist internalization under normal conditions. In other words, cells must overcome higher energetic barriers to deform the membrane and form vesicles large enough to engulf such particles (Lipowsky and Döbereiner, 1998; Roiter et al., 2008).

Interestingly, these internalization profiles change when cells are exposed to osmotic shock (Fig. 3**a**). Notably, cell exposure to hypotonic shock significantly enhanced the internalization efficiency of both P100 and P500, whereas a hypertonic environment did not significantly impact intracellular delivery efficacy. Specifically, hypotonic shock resulted in an approximately 3-fold increase in the cell internalization of P100 compared to cells cultured in isotonic conditions (Fig. 3**b**). The increase of P500 uptake was even larger, achieving approximately a 5-fold increase in HeLa cells under hypotonic conditions if compared to isotonic conditions (Fig. 3**c**). In contrast, hypertonic media did not affect the internalization of particles of any size ($p > 0.05$).

Therefore, hypotonic shock notably enhanced the internalization efficiency of larger NPs. During osmotic shock, membrane rigidity decreases as the cell swells and the plasma membrane stretches, making it more deformable (Stewart et al., 2016). This reduction in rigidity lowers the energy required for particle uptake, facilitating the internalization of larger particles that would otherwise be inefficiently internalized via endocytosis (Muro, 2012; Park and Oh, 2014). Conversely, smaller particles like P100, being more compatible with traditional endocytosis mechanisms, experience less pronounced benefits from the changes induced by osmotic shock.

To the best of our knowledge, we are the first to point out such an improvement of particles uptake through a short-lived (30-min) hypotonic trigger, with no detriment on cell viability. Previous studies have documented the use of hypotonic shocks of short duration for the intracellular delivery of small molecules, including fluorescein (Model

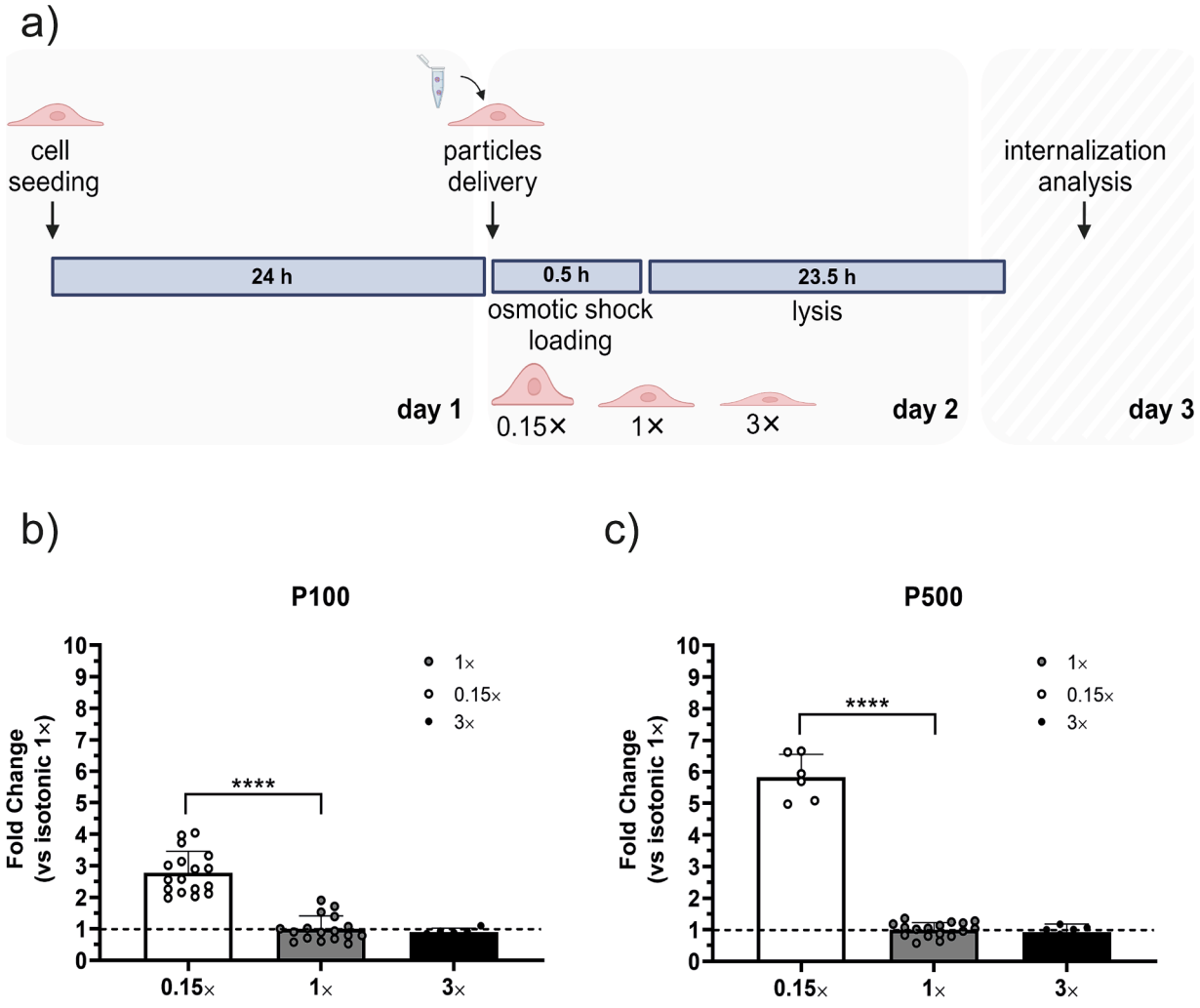

Fig. 3. a) Protocol used to apply osmotic shock to cells and deliver particles (upward configuration). Twenty-four h-post seeding, cells were simultaneously challenged with osmotic shock and particles for 30 min by diluting the culture medium. After the incubation in standard conditions, cells were washed 3 times and lysed. (Image created with Biorender.com) **b)** Assessment of P100 and **c)** P500 internalization in HeLa cells exposed to different osmotic shocks. Results are expressed as mean ± SD ($n \geq 6$, **** $p \leq 0.0001$).

et al., 2022), dextrans (Van der Wijk et al., 2003), and proteins (up to 28 kDa, with an upper threshold size of a few nm in D_H) (Klabusay et al., 2015; Koberna et al., 1999).

Given the intriguing and promising results, we aimed to shed more light on the mechanism behind the tonicity-driven internalization of particles into cells. Various pathways play a role in the internalization of particles, both micro and nano in size (Means et al., 2022; Sahay et al., 2010). The specific endocytic pathway followed by particles, i.e., phagocytosis and pinocytosis, depends on different factors, such as the physicochemical properties of the particles, their interaction with the cell, and the signaling cascades that trigger various structural alterations on the cell surface (Sousa de Almeida et al., 2021). Phagocytosis encompasses the uptake of large particles (D_H > 500 μm) and is only performed by specialized, immune system cells. Pinocytosis occurs in almost every eukaryotic cell and is associated with fluid-phase uptake, and includes macropinocytosis, clathrin-mediated endocytosis, caveolin-mediated endocytosis, and clathrin/caveolae-independent endocytosis (Canton and Battaglia, 2012; Di Fiore and von Zastrow, 2014; Doherty and McMahon, 2009; Kumari et al., 2010). Given that endocytosis is essentially a plasma membrane remodeling mechanism, conditions altering plasma membrane tension are expected to influence the efficiency of cell internalization of objects. As elevated membrane tension makes it more difficult for the membrane to deform, hypotonic conditions have been found to prevent endocytosis. Hypotonic stress can be counteracted to some extent by the actin cytoskeleton in such a way that endocytosis continues even under increased membrane tension (Boulant et al., 2011; Kaplan et al., 2022). On the other hand, although hypertonic conditions would have been expected to raise endocytosis, this has been refuted by our experimental observations. A possible explanation is that cell shrinkage induces cytosolic acidification and increases the concentration of proteins and divalent cations, which, in turn, would impair endocytosis (López-Hernández et al., 2020; Pintsch et al., 2001).

We thus investigated whether cell swelling and cell volume recovery that occur in response to hypotonic conditions may improve the cell uptake of particles. Ad-hoc experiments were carried out according to the two experimental set-ups named “pre-swelling” and “post-swelling” (Fig. 4**a**), depending on the timing of the delivery of particles to the cells and the application of the hypotonic shock (0.15 × medium). In the “pre-swelling” configuration, cells were initially swollen for 5 min (as depicted in Fig. 2) before being exposed to P500 for an additional 25 min. Conversely, in the “post-swelling” setup, cells were simultaneously swollen and added with P500 for 30 min, mirroring the experimental design shown in Fig. 3**a**. The results presented in Fig. 4**a** reveal that in both configurations, the uptake of P500 was significantly higher in swollen cells as compared to the isotonic control ($p < 0.05$). Importantly, the uptake of particles happened during cell swelling ($p > 0.05$ vs 0.15 × pre-swelling vs post-swelling).

Overall, these findings suggest that RVD may be the primary mechanism responsible for increased particle uptake during hypotonic shock. This could be ascribed to the timely deployment of various mechanisms during the RVD phase which aim to reshape the plasma membrane and counteract the heightened membrane tension caused by hypotonic shock (Chadwick et al., 2021).

It has long been recognized that plasma membrane tension plays a crucial role in controlling cell membrane trafficking. Of note, a transient increase in plasma membrane tension orchestrates the activation of exocytosis (Bajno et al., 2000; Gauthier et al., 2011), while its sudden decrease triggers endocytic pathways (Chadwick et al., 2021; Sønder et al., 2021). In this case, both (clathrin-independent) endocytic pathways (CLIC/GEEC) and macropinocytosis are initiated by the reduction of membrane tension, which results in the invagination of cargo (in the case of CLIC/GEEC), and membrane ruffling (in macropinocytosis) (Holst et al., 2017b; Lin and Liu, 2019; Loh et al., 2019; Redpath et al., 2020; Thottacherry et al., 2018; Vidal-Quadras et al., 2017).

To investigate whether the increased cell uptake in the hypotonic environment (Figs. 3 and 4) was due to active endocytosis, we conducted further research. To achieve this, we repeated the internalization experiments in hypotonic conditions now at low temperatures to inhibit energy-dependent endocytosis pathways (clathrin-dependent endocytosis, caveolae-dependent endocytosis, and macropinocytosis) (Nagai et al., 2019). As expected, ice-cold treatment of cells in culture resulted in a significant decrease in NPs uptake, with no effect on cell viability (**Figures S5a-b**). Specifically, we observed an approximately 80 % reduction in NP uptake in CTRL cells treated with P500 at 4 °C vs 37 °C. Conversely, we found that NP uptake under the 0.15× hypotonic condition was temperature-independent (Fig. 4**b**). This suggests that endocytic activity played a minor role while plasma membrane destabilization was the primary mechanism responsible for NP internalization.

These findings hold significant promise, demonstrating that hypotonic treatment effectively enhances cargo uptake in challenging cells. This treatment has the potential to modulate the endocytic process and improve the intracellular delivery efficiency of any kind of cargo.

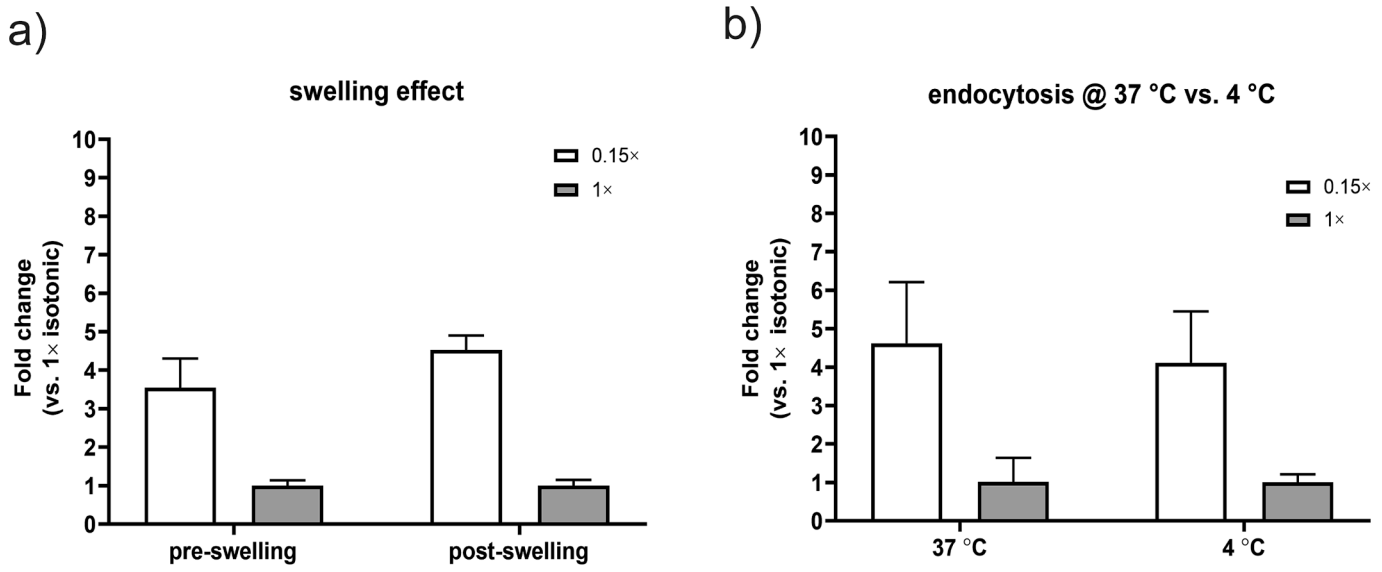

Fig. 4. a) Dependence of P500 internalization in HeLa cells on the swell state of cells (pre- vs post-swelling configuration). **b)** Dependence of P500 internalization in HeLa cells on the temperature (4 °C vs 37 °C). Results are expressed as mean ± SD (n ≥ 3).

Additional particle delivery experiments were purposefully designed to gain deeper insights into the cellular mechanisms responsible for particle uptake under hypotonic conditions. To rule out the possibility of particle sedimentation being the cause for the observed increase in uptake, two distinct setups termed upward and upside-down were utilized.

Fig. 5 demonstrates that the internalization mechanisms induced by osmotic shock are independent of particle sedimentation. Notably, no statistical differences were observed between the upside-down and upright layouts under isotonic conditions ($p > 0.05$), confirming that variations in NPs uptake rely on their inherent characteristics (**Figure S6**).

Altogether, these findings disclose hypotonic shock as an effective means to enhance intracellular delivery of NPs. This approach could be effective in contexts beyond *in vitro*, where the gravitational settling of cargoes would not be responsible for increasing their concentration at the cell-medium interface and facilitating their uptake (Alexander et al., 2013; Hinderliter et al., 2010; Liyanage et al., 2016; Midelet et al., 2017; Zheng et al., 2019).

3.3. *Hypotonic shock increases the uptake of small therapeutic cargos in relevant cells*

The investigation of the osmotic shock mechanism paved the way for its further implementation in relevant cellular models. This sequential approach facilitates the exploration of its potential to ease the intracellular delivery of different cargoes.

We first evaluated the effect of the hypotonic shock on NP uptake. Similarly to what was observed in HeLa cells, exposure to hypotonic shock significantly enhanced P100 and P500 internalization by approximately 3-fold and 10-fold, compared to the isotonic control (Fig. 6**a, b**). These findings highlight the effectiveness of hypotonic shock as a potentially universal treatment to enhance cargo uptake into cells.

In light of the above, we hypothesized that we could leverage the hypotonic shock to deliver small therapeutics into relevant cell types, such as hFBs. We thus delivered icerguastat to cells under osmotic shock (Bai et al., 2022; Dalla Bella et al., 2021). Icerguastat, an analogue of guanabenz that lacks α2-adrenergic agonist activity, selectively inhibits endoplasmic reticulum (ER) stress-induced eIF2α-phosphatase, facilitating the clearance of misfolded protein. This mechanism plays a critical role in the ALS pathogenesis by altering proteostasis regulation (Kanekura et al., 2009; Maharjan and Saxena, 2016; Parakh and Atkin, 2016). ATF4, a transcription factor in ER stress pathways, regulates both adaptive and apoptotic mechanisms. Its activity is modulated by miR-106b-5p, which leads to ATF4 gene activation and promotes the expression of cytoprotective genes, supporting adaptive responses and cell survival. In a recent multicenter, randomized, double-blind phase 2 clinical trial (PROMISE), guanabenz demonstrated a speciifically effective and dose-dependent response in bulbar onset ALS patients compared to those with spinal onset and placebo patients (Dalla Bella et al., 2021b). Notably, miR-106b-5p was identified as a biomarker associated with the pharmacological modulation of the unfolded protein response by both guanabenz and icerguastat in patients with bulbar onset ALS (Marcuzzo et al., 2024). To investigate the potential role of hypotonic shock in enhancing icerguastat internalization and function, we measured the expression levels of miR-106b-5p in hFbs (i.e., basal) derived from bulbar onset ALS patients. The expression levels of miR-106b-5p were significant lower in untreated ALS compared to CTRL (healthy) hFBs (Fig. 6**c**).ALS-hFBs were treated with 10 nM icerguastat for 30 min in both hypotonic and isotonic condition (osmotic stimulation time: 30 min) (Fig. 6**c**). Surprisingly, ALS-hFBs exposed to hypotonic shock in combination with icerguastat showed a significant increase in the expression levels of miR-106b-5p after treatment compared to untreated ALS cells, normalizating to the reference level.

Overall, our findings demonstrated that hypotonic conditions enhance delivery efficiency, which we sleveraged to increase the uptake of a therapeutic drug (icerguastat) in ALShFBs (Bai et al., 2022; Dalla Bella et al., 2021). Osmotic shock emergess as a promising strategy to improve intracellular drug delivery and potentially enhance the delivery in tissues. However, the technique may be more effective and safer in certain contexts, such as localized drug delivery in muscles or skin, while requiring careful control in more sensitive tissues like the brain or

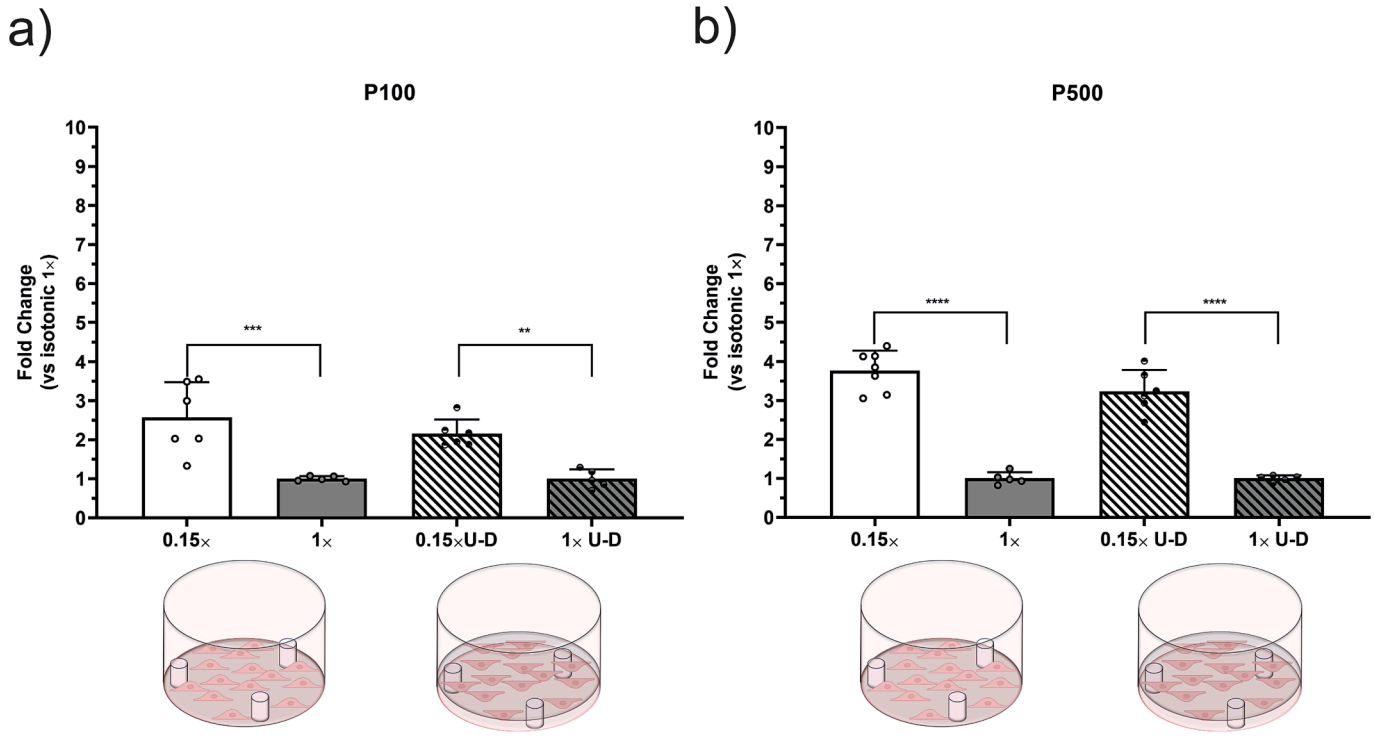

Fig. 5. a) Evaluation of P100 and **b)** P500 internalization in HeLa cells exposed to hypotonic shock in standard and upside-down conditions. Results are expressed as mean ± SD ($n \geq 6$, ** $p \leq 0.01$, *** $p \leq 0.001$, **** $p \leq 0.0001$).

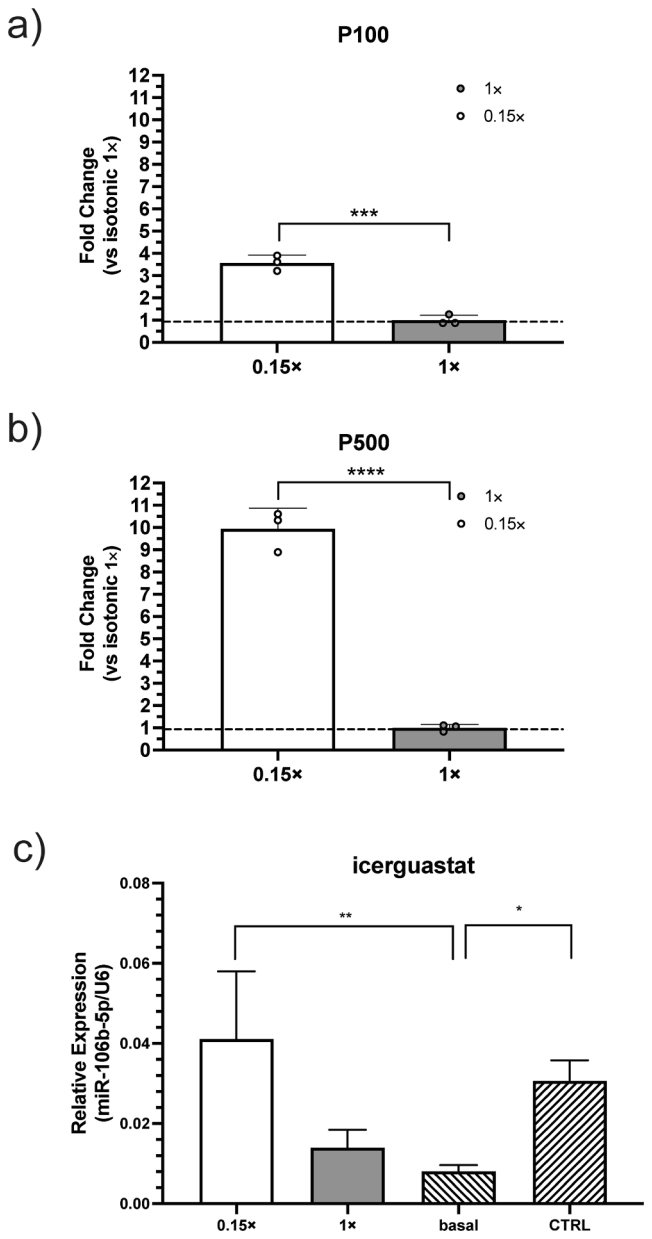

Fig. 6. a) Evaluation of P100 and **b)** P500 internalization in hFBs exposed to different osmotic media (n = 3). **c)** Relative expression of miR-106-5p in bulbar onset ALS fibroblast (basal condition) after the administration of icerguastat in i) 30 min-long hypotonic shock (0.15×), ii) 30 min-long isotonic condition(1×). CTRL refers to the miR-106b-5p content in healthy control hFBs. RT-PCR analysis of miR-106b-5p in total RNA extracted from hFBs. Data are expressed as mean ± SD (n ≥ 5, *p < 0.05).

kidneys. Further investigation into these tissue-specific responses is cruciaal to optimize therapeutic potential of osmotic shock.

4. Conclusions

In this study, hypotonic shock was utilized as a trigger to enhance the cellular uptake of (nano)cargoes. This strategy proved to be a straightforward and rapid method to improve the internalization of (nano)cargos into cells through the modulation of cell membrane tension in response to hypotonic-induced swelling. Importantly, it was observed that the mechanisms ruling internalization trafficking after the osmotic shock are independent of active endocytic mechanisms, thus making hypotonic stimulus particularly attractive for cells somewhat refractory to internalize cargoes, such as primary cells.

The protocol developed to stimulate cells is highly adaptable to the operator's needs, enabling the rapid delivery of cargo molecules and nano-sized materials in an aqueous solution.

The simplicity of the osmotic shock method makes it particularly appealing for enhancing cell internalization of (nano)cargoes *in vivo*, especially in specific contexts such as dermal or intramuscular injections, including vaccines. In these situations, transiently modifying osmotic tension locally may facilitate drug absorption and improve therapeutic efficacy. By enhancing drug uptake, providing a non-invasive delivery method, and enabling localized treatment, this approach could significantly enhance the overall efficacy of therapeutic interventions while reducing the systemic side effects associated with conventional drug administration.

Further studies are necessary to establish safe protocols and determine the optimal parameters for applying osmotic shock across various therapeutic contexts, ensuring that the benefits of enhanced drug uptake outweigh the associated risks. These pre-clinical studies will be instrumental in identifying optimal drug dosages, administration routes, and potential side effects in a more biologically relevant context.

CRediT authorship contribution statement

Beatrice Ruzzante: Writing – review & editing, Writing – original draft, Visualization, Validation, Software, Methodology, Investigation, Data curation, Conceptualization. **Flaminia Fruzzetti:** Writing – review & editing, Visualization, Investigation, Data curation. **Marco Cattaneo:** Writing – review & editing, Visualization, Validation, Investigation. **Giuseppe Lauria Pinter:** Writing – review & editing, Visualization, Validation. **Stefania Marcuzzo:** Writing – review & editing, Visualization, Validation. **Gabriele Candiani:** Writing – review & editing, Visualization, Validation, Methodology, Conceptualization. **Nina Bono:** Writing – review & editing, Writing – original draft, Visualization, Supervision, Methodology, Formal analysis, Data curation, Conceptualization.

Declaration of competing interest

The authors declare that they have no known competing financial interests or personal relationships that could have appeared to influence the work reported in this paper.

Acknowledgements

The authors would like to thank InFlectis Bioscience for kindly providing icerguastat, Mr. Paolo Tarsini for technical support, Politecnico di Milano and Italian Ministry of Health (RCC) for financial support. This work was supported by TRANS-ALS (grant no. 2015-0023 to G.L.) and INTERSLA (grant no. 1157625 to G.L.).

Illustrations in Figures were created with BioRender.com

Appendix A. Supplementary data

Supplementary data to this article can be found online at https://doi.org/10.1016/j.ijpharm.2024.125008.

Data availability

Data will be made available on request.

References

Adar, R.M., Vishen, A.S., Joanny, J.-F., Sens, P., Safran, S.A., 2022. Volume regulation in adhered cells: roles of surface tension and cell swelling. doi: 10.1101/2022.08.24.505072.

Akatay, A.A., Wu, T., Djakbarova, U., Thompson, C., Cocucci, E., Zandi, R., Rudnick, J., Kural, C., 2022. Endocytosis at extremes: Formation and internalization of giant

clathrin-coated pits under elevated membrane tension. Front. Mol. Biosci. 9. https://doi.org/10.3389/fmolb.2022.959737.
Alexander, C.M., Dabrowiak, J.C., Goodisman, J., 2013. Gravitational sedimentation of gold nanoparticles. J. Colloid Interface Sci. 396, 53–62. https://doi.org/10.1016/j.jcis.2013.01.005.
Alexander, R.T., Grinstein, S., 2006. Na^+/H^+ exchangers and the regulation of volume. Acta Physiol. 187, 159–167. https://doi.org/10.1111/j.1748-1716.2006.01558.x.
Ayee, M.A.A., LeMaster, E., Teng, T., Lee, J., Levitan, I., 2018. Hypotonic challenge of endothelial cells increases membrane stiffness with no effect on tether force. Biophys. J. 114, 929–938. https://doi.org/10.1016/j.bpj.2017.12.032.
Bai, Y., Treins, C., Volpi, V.G., Scapin, C., Ferri, C., Mastrangelo, R., Touvier, T., Florio, F., Bianchi, F., Del Carro, U., Baas, F.F., Wang, D., Miniou, P., Guedat, P., Shy, M.E., D'Antonio, M., 2022. Treatment with IFB-088 Improves Neuropathy in CMT1A and CMT1B Mice. Mol. Neurobiol. 59, 4159–4178. https://doi.org/10.1007/s12035-022-02838-y.
Bajno, L., Peng, X.-R., Schreiber, A.D., Moore, H.-P., Trimble, W.S., Grinstein, S., 2000. Focal exocytosis of Vamp3-containing vesicles at sites of phagosome formation. J. Cell Biol. 149, 697–706. https://doi.org/10.1083/jcb.149.3.697.
Biswas, P., Ray, D., Jana, S., Das, J., Sinha, B., Sinha, D.K., 2022. Probing the role of macromolecular crowding in cell volume regulation using fluorescence anisotropy. doi: 10.1101/2022.04.07.487477.
Bono, N., Ponti, F., Mantovani, D., Candiani, G., 2020. Non-viral in vitro gene delivery: It is now time to set the bar! Pharmaceutics 12, 183. https://doi.org/10.3390/pharmaceutics12020183.
Boulant, S., Kural, C., Zeeh, J.-C., Ubelmann, F., Kirchhausen, T., 2011. Actin dynamics counteract membrane tension during clathrin-mediated endocytosis. Nat. Cell Biol. 13, 1124–1131. https://doi.org/10.1038/ncb2307.
Brooks, B.R., Miller, R.G., Swash, M., Munsat, T.L., 2000. El Escorial revisited: Revised criteria for the diagnosis of amyotrophic lateral sclerosis. Amyotroph. Lateral Scler. Other Motor Neuron Disord. 1, 293–299. https://doi.org/10.1080/146608200300079536.
Canton, I., Battaglia, G., 2012. Endocytosis at the nanoscale. Chem. Soc. Rev. 41, 2718. https://doi.org/10.1039/c2cs15309b.
Chadwick, S.R., Wu, J.-Z., Freeman, S.A., 2021. Solute transport controls membrane tension and organellar volume. Cell. Physiol. Biochem. 55, 1–24. https://doi.org/10.33594/000000318.
Chou, L.Y.T., Ming, K., Chan, W.C.W., 2011. Strategies for the intracellular delivery of nanoparticles. Chem. Soc. Rev. 40, 233–245. https://doi.org/10.1039/C0CS00003E.
Corbo, C., Molinaro, R., Parodi, A., Toledano Furman, N.E., Salvatore, F., Tasciotti, E., 2016. The impact of nanoparticle protein corona on cytotoxicity, immunotoxicity and target drug delivery. Nanomedicine 11, 81–100. https://doi.org/10.2217/nnm.15.188.
Dai, J., Sheetz, M.P., Wan, X., Morris, C.E., 1998. Membrane tension in swelling and shrinking molluscan neurons. J. Neurosci. 18, 6681–6692. https://doi.org/10.1523/JNEUROSCI.18-17-06681.1998.
Dalla Bella, E., Bersano, E., Antonini, G., Borghero, G., Capasso, M., Caponnetto, C., Chiò, A., Corbo, M., Filosto, M., Giannini, F., Spataro, R., Lunetta, C., Mandrioli, J., Messina, S., Monsurrò, M.R., Mora, G., Riva, N., Rizzi, R., Siciliano, G., Silani, V., Simone, I., Sorarù, G., Tugnoli, V., Verriello, L., Volanti, P., Furlan, R., Nolan, J.M., Abgueguen, E., Tramacere, I., Lauria, G., 2021. The unfolded protein response in amyotrophic later sclerosis: Results of a phase 2 trial. Brain 144, 2635–2647. https://doi.org/10.1093/brain/awab167.
Di Fiore, P.P., von Zastrow, M., 2014. Endocytosis, signaling, and beyond. Cold Spring Harb. Perspect. Biol. 6, a016865–a. https://doi.org/10.1101/cshperspect.a016865.
Diz-Muñoz, A., Thurley, K., Chintamen, S., Altschuler, S.J., Wu, L.F., Fletcher, D.A., Weiner, O.D., 2016. Membrane tension acts through PLD2 and mTORC2 to limit actin network assembly during neutrophil migration. PLoS Biol. 14, e1002474. https://doi.org/10.1371/journal.pbio.1002474.
Djakbarova, U., Madraki, Y., Chan, E.T., Kural, C., 2021. Dynamic interplay between cell membrane tension and clathrin-mediated endocytosis. Biol. Cell 113, 344–373. https://doi.org/10.1111/boc.202000110.
Doherty, G.J., McMahon, H.T., 2009. Mechanisms of endocytosis. Annu. Rev. Biochem 78, 857–902. https://doi.org/10.1146/annurev.biochem.78.081307.110540.
Fajrial, A.K., Liu, K., Gao, Y., Gu, J., Lakerveld, R., Ding, X., 2021. Characterization of single-cell osmotic swelling dynamics for new physical biomarkers. Anal. Chem. 93, 1317–1325. https://doi.org/10.1021/acs.analchem.0c02289.
Fletcher, D.A., Mullins, R.D., 2010. Cell mechanics and the cytoskeleton. Nature 463, 485–492. https://doi.org/10.1038/nature08908.
Fröhlich, E., Samberger, C., Kueznik, T., Absenger, M., Roblegg, E., Zimmer, A., Pieber, T.R., 2009. Cytotoxicity of nanoparticles independent from oxidative stress. J. Toxicol. Sci. 34, 363–375. https://doi.org/10.2131/jts.34.363.
Gao, J., Karp, J.M., Langer, R., Joshi, N., 2023. The future of drug delivery. Chem. Mater. 35, 359–363. https://doi.org/10.1021/acs.chemmater.2c03003.
Gauthier, N.C., Fardin, M.A., Roca-Cusachs, P., Sheetz, M.P., 2011. Temporary increase in plasma membrane tension coordinates the activation of exocytosis and contraction during cell spreading. Proc. Natl. Acad. Sci. 108, 14467–14472. https://doi.org/10.1073/pnas.1105845108.
Gauthier, N.C., Masters, T.A., Sheetz, M.P., 2012. Mechanical feedback between membrane tension and dynamics. Trends Cell Biol. 22, 527–535. https://doi.org/10.1016/j.tcb.2012.07.005.
Ghisleni, A., Gauthier, N.C., 2024. Mechanotransduction through membrane tension: It's all about propagation? Curr. Opin. Cell Biol. 86, 102294. https://doi.org/10.1016/j.ceb.2023.102294.
Gratton, S.E.A., Ropp, P.A., Pohlhaus, P.D., Luft, J.C., Madden, V.J., Napier, M.E., DeSimone, J.M., 2008. The effect of particle design on cellular internalization pathways. Proc. Natl. Acad. Sci. 105, 11613–11618. https://doi.org/10.1073/pnas.0801763105.
Guilak, F., Erickson, G.R., Ting-Beall, H.P., 2002. The effects of osmotic stress on the viscoelastic and physical properties of articular chondrocytes. Biophys. J. 82, 720–727. https://doi.org/10.1016/S0006-3495(02)75434-9.
Guo, M., Pegoraro, A.F., Mao, A., Zhou, E.H., Arany, P.R., Han, Y., Burnette, D.T., Jensen, M.H., Kasza, K.E., Moore, J.R., Mackintosh, F.C., Fredberg, J.J., Mooney, D.J., Lippincott-Schwartz, J., Weitz, D.A., 2017. Cell volume change through water efflux impacts cell stiffness and stem cell fate. Proceedings of the National Academy of Sciences 114. doi: 10.1073/pnas.1705179114.
Hinderliter, P.M., Minard, K.R., Orr, G., Chrisler, W.B., Thrall, B.D., Pounds, J.G., Teeguarden, J.G., 2010. ISDD: A computational model of particle sedimentation, diffusion and target cell dosimetry for in vitro toxicity studies. Part. Fibre Toxicol. 7, 36. https://doi.org/10.1186/1743-8977-7-36.
Hoffmann, E.K., Lambert, I.H., Pedersen, S.F., 2009. Physiology of cell volume regulation in vertebrates. Physiol. Rev. 89, 193–277. https://doi.org/10.1152/physrev.00037.2007.
Holst, M.R., Vidal-Quadras, M., Larsson, E., Song, J., Hubert, M., Blomberg, J., Lundborg, M., Landström, M., Lundmark, R., 2017. Clathrin-independent endocytosis suppresses cancer cell blebbing and invasion. Cell Rep. 20, 1893–1905. https://doi.org/10.1016/j.celrep.2017.08.006.
Kanekura, K., Suzuki, H., Aiso, S., Matsuoka, M., 2009. ER stress and unfolded protein response in amyotrophic lateral sclerosis. Mol. Neurobiol. 39, 81–89. https://doi.org/10.1007/s12035-009-8054-3.
Kaplan, C., Kenny, S.J., Chen, X., Schöneberg, J., Sitarska, E., Diz-Muñoz, A., Akamatsu, M., Xu, K., Drubin, D.G., 2022. Load adaptation by endocytic actin networks. Mol. Biol. Cell 33. https://doi.org/10.1091/mbc.E21-11-0589.
Klabusay, M., Skopalík, J., Erceg, S., Hrdlička, A., 2015. Aequorin as intracellular Ca2+ indicator incorporated in follicular lymphoma cells by hypoosmotic shock treatment. Folia Biol. (Praha) 61, 134–139.
Koberna, K., Staněk, D., Malínský, J., Eltsov, M., Pliss, A., Čtrnáctá, V., Cermanová, Š., Raška, I., 1999. Nuclear organization studied with the help of a hypotonic shift: its use permits hydrophilic molecules to enter into living cells. Chromosoma 108, 325–335. https://doi.org/10.1007/s004120050384.
Kumari, S., MG, S., Mayor, S., 2010. Endocytosis unplugged: multiple ways to enter the cell. Cell Res 20, 256–275. doi: 10.1038/cr.2010.19.
Lang, F., 2007. Mechanisms and significance of cell volume regulation. J. Am. Coll. Nutr. 26, 613S–623S. https://doi.org/10.1080/07315724.2007.10719667.
Lin, S.-S., Liu, Y.-W., 2019. Mechanical stretch induces mTOR recruitment and activation at the phosphatidic acid-enriched macropinosome in muscle cell. Front. Cell Dev. Biol. 7. https://doi.org/10.3389/fcell.2019.00078.
Lipowsky, R., Döbereiner, H.-G., 1998. Vesicles in contact with nanoparticles and colloids. Europhys. Lett. (EPL) 43, 219–225. https://doi.org/10.1209/epl/i1998-00343-4.
Liyanage, D.D., Thamali, R.J.K.A., Kumbalatara, A.A.K., Weliwita, J.A., Witharana, S., 2016. An analysis of nanoparticle settling times in liquids. J. Nanomater. 2016, 1–7. https://doi.org/10.1155/2016/7061838.
Loh, J., Chuang, M.-C., Lin, S.-S., Joseph, J., Su, Y.-A., Hsieh, T.-L., Chang, Y.-C., Liu, A. P., Liu, Y.-W., 2019. An acute decrease in plasma membrane tension induces macropinocytosis via PLD2 activation. J. Cell Sci. 132. https://doi.org/10.1242/jcs.232579.
López-Hernández, T., Haucke, V., Maritzen, T., 2020. Endocytosis in the adaptation to cellular stress. Cell Stress 4, 230–247. https://doi.org/10.15698/cst2020.10.232.
Lunov, O., Syrovets, T., Loos, C., Beil, J., Delacher, M., Tron, K., Nienhaus, G.U., Musyanovych, A., Mailänder, V., Landfester, K., Simmet, T., 2011. Differential uptake of functionalized polystyrene nanoparticles by human macrophages and a monocytic cell line. ACS Nano 5, 1657–1669. https://doi.org/10.1021/nn2000756.
Maharjan, N., Saxena, S., 2016. ER strikes again: Proteostasis dysfunction in ALS. EMBO J. 35, 798–800. https://doi.org/10.15252/embj.201694117.
Mang, T., Lindemann, S., Gigout, A., 2020. Increasing the medium osmolarity reduces the inflammatory status of human OA chondrocytes and increases their responsiveness to GDF-5. Int. J. Mol. Sci. 21, 531. https://doi.org/10.3390/ijms21020531.
Mann, S.K., Czuba, E., Selby, L.I., Such, G.K., Johnston, A.P.R., 2016. Quantifying nanoparticle internalization using a high throughput internalization assay. Pharm. Res. 33, 2421–2432. https://doi.org/10.1007/s11095-016-1984-3.
Mao, F., Yang, Y., Jiang, H., 2021. Endocytosis and exocytosis protect cells against severe membrane tension variations. Biophys. J. 120, 5521–5529. https://doi.org/10.1016/j.bpj.2021.11.019.
Marcuzzo, S., Salvi, E., Dalla Bella, E., Perico, D., De Palma, A., Mauri, P., Lauria Pinter, G., 2024. Microrna as a diagnostic tool and for developing advanced therapies of amyotrophic lateral sclerosis (ALS) with bulbar onset. 102023000009462.
Means, N., Elechalawar, C.K., Chen, W.R., Bhattacharya, R., Mukherjee, P., 2022. Revealing macropinocytosis using nanoparticles. Mol. Aspects Med. 83, 100993. https://doi.org/10.1016/j.mam.2021.100993.
Midelet, J., El-Sagheer, A.H., Brown, T., Kanaras, A.G., Werts, M.H.V., 2017. The sedimentation of colloidal nanoparticles in solution and its study using quantitative digital photography. Part. Part. Syst. Char. 34. https://doi.org/10.1002/ppsc.201700095.
Model, M.A., Hassani Nia, F., Zook, E., Hollembeak, J.E., Stauber, T., 2022. Uptake of fluorescein upon osmotic cell swelling is dependent on the volume- regulated anion channel VRAC/LRRC8. Paracelsus Proc. Exp. Med. 1, 3–14. https://doi.org/10.33594/000000533.
Monti, D.M., Guarnieri, D., Napolitano, G., Piccoli, R., Netti, P., Fusco, S., Arciello, A., 2015. Biocompatibility, uptake and endocytosis pathways of polystyrene

nanoparticles in primary human renal epithelial cells. J. Biotechnol. 193, 3–10. https://doi.org/10.1016/j.jbiotec.2014.11.004.
Morshedi Rad, D., Alsadat Rad, M., Razavi Bazaz, S., Kashaninejad, N., Jin, D., Ebrahimi Warkiani, M., 2021. A comprehensive review on intracellular delivery. Adv. Mater. 33. https://doi.org/10.1002/adma.202005363.
Muro, S., 2012. Challenges in design and characterization of ligand-targeted drug delivery systems. J. Control. Release 164, 125–137. https://doi.org/10.1016/j.jconrel.2012.05.052.
Nagai, N., Ogata, F., Otake, H., Nakazawa, Y., Kawasaki, N., 2019. Energy-dependent endocytosis is responsible for drug transcorneal penetration following the instillation of ophthalmic formulations containing indomethacin nanoparticles . Int. J. Nanomed. 14, 1213–1227. https://doi.org/10.2147/IJN.S196681.
Nowak, M., Brown, T.D., Graham, A., Helgeson, M.E., Mitragotri, S., 2020. Size, shape, and flexibility influence nanoparticle transport across brain endothelium under flow. Bioeng. Transl. Med. 5. https://doi.org/10.1002/btm2.10153.
Ozturk, S.S., Palsson, B.O., 1991. Effect of medium osmolarity on hybridoma growth, metabolism, and antibody production. Biotechnol. Bioeng. 37, 989–993. https://doi.org/10.1002/bit.260371015.
Pan, L., Zhang, P., Hu, F., Yan, R., He, M., Li, W., Xu, J., Xu, K., 2019. Hypotonic stress induces fast, reversible degradation of the vimentin cytoskeleton via intracellular calcium release. Adv. Sci. 6. https://doi.org/10.1002/advs.201900865.
Parakh, S., Atkin, J.D., 2016. Protein folding alterations in amyotrophic lateral sclerosis. Brain Res. 1648, 633–649. https://doi.org/10.1016/j.brainres.2016.04.010.
Park, J.H., Oh, N., 2014. Endocytosis and exocytosis of nanoparticles in mammalian cells. Int. J. Nanomed. 51. https://doi.org/10.2147/IJN.S26592.
Peckys, D., Mazur, P., 2012. Regulatory volume decrease in COS-7 cells at 22 °C and its influence on the Boyle van't Hoff relation and the determination of the osmotically inactive volume. Cryobiology 65, 74–78. https://doi.org/10.1016/j.cryobiol.2012.03.008.
Pezzoli, D., Giupponi, E., Mantovani, D., Candiani, G., 2017. Size matters for in vitro gene delivery: investigating the relationships among complexation protocol, transfection medium, size and sedimentation. Sci. Rep. 7, 44134. https://doi.org/10.1038/srep44134.
Pintsch, T., Satre, M., Klein, G., Martin, J.-B., Schuster, S.C., 2001. Cytosolic acidification as a signal mediating hyperosmotic stress responses in Dictyostelium discoideum. BMC Cell Biol. 2, 9. https://doi.org/10.1186/1471-2121-2-9.
Pontes, B., Monzo, P., Gauthier, N.C., 2017. Membrane tension: A challenging but universal physical parameter in cell biology. Semin. Cell Dev. Biol. 71, 30–41. https://doi.org/10.1016/j.semcdb.2017.08.030.
Ponti, F., Bono, N., Russo, L., Bigini, P., Mantovani, D., Candiani, G., 2022. Vibropolyfection: coupling polymer-mediated gene delivery to mechanical stimulation to enhance transfection of adherent cells. J. Nanobiotechnol. 20, 363. https://doi.org/10.1186/s12951-022-01571-x.
Ray, M., Lee, Y.-W., Scaletti, F., Yu, R., Rotello, V.M., 2017. Intracellular delivery of proteins by nanocarriers. Nanomedicine 12, 941–952. https://doi.org/10.2217/nnm-2016-0393.
Redpath, G.M.I., Betzler, V.M., Rossatti, P., Rossy, J., 2020. Membrane heterogeneity controls cellular endocytic trafficking. Front. Cell Dev. Biol. 8. https://doi.org/10.3389/fcell.2020.00757.
Roffay, C., Molinard, G., Kim, K., Urbanska, M., Andrade, V., Barbarasa, V., Nowak, P., Mercier, V., García-Calvo, J., Matile, S., Loewith, R., Echard, A., Guck, J., Lenz, M., Roux, A., 2021a. Passive coupling of membrane tension and cell volume during active response of cells to osmosis. Proceedings of the National Academy of Sciences 118. doi: 10.1073/pnas.2103228118.
Roiter, Y., Ornatska, M., Rammohan, A.R., Balakrishnan, J., Heine, D.R., Minko, S., 2008. Interaction of nanoparticles with lipid membrane. Nano Lett. 8, 941–944. https://doi.org/10.1021/nl080080l.
Sahay, G., Alakhova, D.Y., Kabanov, A.V., 2010. Endocytosis of nanomedicines. J. Control. Release 145, 182–195. https://doi.org/10.1016/j.jconrel.2010.01.036.
Sieber, S., Michaelis, M., Gühring, H., Lindemann, S., Gigout, A., 2020. Importance of osmolarity and oxygen tension for cartilage tissue engineering. Biores. Open Access 9, 106–115. https://doi.org/10.1089/biores.2020.0009.
Sinha, B., Köster, D., Ruez, R., Gonnord, P., Bastiani, M., Abankwa, D., Stan, R.V., Butler-Browne, G., Vedie, B., Johannes, L., Morone, N., Parton, R.G., Raposo, G., Sens, P., Lamaze, C., Nassoy, P., 2011. Cells respond to mechanical stress by rapid disassembly of caveolae. Cell 144, 402–413. https://doi.org/10.1016/j.cell.2010.12.031.
Sitarska, E., Diz-Muñoz, A., 2020. Pay attention to membrane tension: Mechanobiology of the cell surface. Curr. Opin. Cell Biol. 66, 11–18. https://doi.org/10.1016/j.ceb.2020.04.001.
Sønder, S.L., Häger, S.C., Heitmann, A.S.B., Frankel, L.B., Dias, C., Simonsen, A.C., Nylandsted, J., 2021. Restructuring of the plasma membrane upon damage by LC3-associated macropinocytosis. Sci. Adv. 7. https://doi.org/10.1126/sciadv.abg1969.
Sousa de Almeida, M., Susnik, E., Drasler, B., Taladriz-Blanco, P., Petri-Fink, A., Rothen-Rutishauser, B., 2021. Understanding nanoparticle endocytosis to improve targeting strategies in nanomedicine. Chem. Soc. Rev. 50, 5397–5434. https://doi.org/10.1039/D0CS01127D.
Stewart, M.P., Sharei, A., Ding, X., Sahay, G., Langer, R., Jensen, K.F., 2016. In vitro and ex vivo strategies for intracellular delivery. Nature 538, 183–192. https://doi.org/10.1038/nature19764.
Stewart, M.P., Langer, R., Jensen, K.F., 2018. Intracellular delivery by membrane disruption: Mechanisms, strategies, and concepts. Chem. Rev. 118, 7409–7531. https://doi.org/10.1021/acs.chemrev.7b00678.
Takai, T., Ohmori, H., 1990. DNA transfection of mouse lymphoid cells by the combination of DEAE-dextran-mediated DNA uptake and osmotic shock procedure. Biochimica et Biophysica Acta (BBA) - Gene Structure and Expression 1048, 105–109. doi: 10.1016/0167-4781(90)90029-2.
Thottacherry, J.J., Kosmalska, A.J., Kumar, A., Vishen, A.S., Elosegui-Artola, A., Pradhan, S., Sharma, S., Singh, P.P., Guadamillas, M.C., Chaudhary, N., Vishwakarma, R., Trepat, X., del Pozo, M.A., Parton, R.G., Rao, M., Pullarkat, P., Roca-Cusachs, P., Mayor, S., 2018. Mechanochemical feedback control of dynamin independent endocytosis modulates membrane tension in adherent cells. Nat. Commun. 9, 4217. https://doi.org/10.1038/s41467-018-06738-5.
Urbaniak, P., Wronski, S., Tarasiuk, J., Lipinski, P., Kotwicka, M., 2022. A new method to estimate 3D cell parameters from 2D microscopy images. Biochimica et Biophysica Acta (BBA) - Molecular Cell Research 1869, 119286. doi: 10.1016/j.bbamcr.2022.119286.
Van der Wijk, T., Tomassen, S.F.B., Houtsmuller, A.B., de Jonge, H.R., Tilly, B.C., 2003. Increased vesicle recycling in response to osmotic cell swelling. J. Biol. Chem. 278, 40020–40025. https://doi.org/10.1074/jbc.M307603200.
Venkova, L., Vishen, A.S., Lembo, S., Srivastava, N., Duchamp, B., Ruppel, A., Williart, A., Vassilopoulos, S., Deslys, A., Garcia Arcos, J.M., Diz-Muñoz, A., Balland, M., Joanny, J.-F., Cuvelier, D., Sens, P., Piel, M., 2022. A mechano-osmotic feedback couples cell volume to the rate of cell deformation. Elife 11. https://doi.org/10.7554/eLife.72381.
Vidal-Quadras, M., Holst, M.R., Francis, M.K., Larsson, E., Hachimi, M., Yau, W.-L., Peränen, J., Martín-Belmonte, F., Lundmark, R., 2017. Endocytic turnover of Rab8 controls cell polarization. J. Cell Sci. 130, 1147–1157. https://doi.org/10.1242/jcs.195420.
Vieira, F.G., Ping, Q., Moreno, A.J., Kidd, J.D., Thompson, K., Jiang, B., Lincecum, J.M., Wang, M.Z., De Zutter, G.S., Tassinari, V.R., Levine, B., Hatzipetros, T., Gill, A., Perrin, S., 2015. Guanabenz treatment accelerates disease in a mutant SOD1 mouse model of ALS. PLoS One 10, e0135570. https://doi.org/10.1371/journal.pone.0135570.
Xu, X., Urban, J.P.G., Tirlapur, U.K., Cui, Z., 2010. Osmolarity effects on bovine articular chondrocytes during three-dimensional culture in alginate beads. Osteoarthritis Cartilage 18, 433–439. https://doi.org/10.1016/j.joca.2009.10.003.
Zanganeh, S., Spitler, R., Erfanzadeh, M., Alkilany, A.M., Mahmoudi, M., 2016. Protein corona: Opportunities and challenges. Int. J. Biochem. Cell Biol. 75, 143–147. https://doi.org/10.1016/j.biocel.2016.01.005.
Zhang, W., Taheri-Ledari, R., Ganjali, F., Mirmohammadi, S.S., Qazi, F.S., Saeidirad, M., KashtiAray, A., Zarei-Shokat, S., Tian, Y., Maleki, A., 2023. Effects of morphology and size of nanoscale drug carriers on cellular uptake and internalization process: A review. RSC Adv. 13, 80–114. https://doi.org/10.1039/D2RA06888E.
Zheng, X., Li, Y., Chen, D., Zheng, A., Que, Q., 2019. Study on analysis and sedimentation of alumina nanoparticles. Int. J. Environ. Res. Public Health 16, 510. https://doi.org/10.3390/ijerph16030510.
Zhu, M., Nie, G., Meng, H., Xia, T., Nel, A., Zhao, Y., 2013. Physicochemical properties determine nanomaterial cellular uptake, transport, and fate. Acc. Chem. Res. 46, 622–631. https://doi.org/10.1021/ar300031y.